Supporting Information

A Novel Stable Zinc-Oxo Cluster for Advanced Lithography Patterning

Youming Si,[a] Yingdong Zhao,[a] Guangyue Shi,[d] Danhong Zhou,[a] Feng Luo,[d] Pengzhong Chen*,[ab] Jiangli Fan*,[ac] and Xiaojun Peng[ac]

[a]State Key Laboratory of Fine Chemicals, Frontiers Science Center for Smart Materials Oriented Chemical Engineering, School of Chemical Engineering, Dalian University of Technology, Dalian 116024, China.

[b]Ningbo Institute of Dalian University of Technology, Ningbo 315016, China

[c]Research Institute of Dalian University of Technology in Shenzhen, Shenzhen 518057, China.

[d]School of Materials Science and Engineering, Nankai University, Tianjin 300350, China.

Materials and methods

All the chemicals and solvents were of reagent grade quality and obtained from commercial sources and used without further purification. Si-substrates, Product: polished, orientation: 100, type: N, are commercially available and directly used without treatment. The elemental analyses of C, H were performed on a UNICUBE elemental analyzer. Thermogravimetric analyses were measured by TA Q600 SDT instrument and recorded under N_2 followed by a ramp of 10 °C min^{-1} up to 800 °C. Zn content was recorded by PerkinElmer Optima 2000DV ICP-AES. ^{1}H NMR and ^{13}C NMR spectra were recorded by a BRUKER 400M and 500M spectrometer, using dimethyl sulfoxide-d$_6$ (DMSO-d_6) or chloroform-d as a solvent with TMS as the internal standard. Mass spectrometric (MS) data were carried out using LTQ Orbitrap XL instruments. The thickness of the films were measured by J.A. Woollam Co INC M-2000V ellipsometer. E-beam lithography were performed on Thermo Fisher ScientificHelios 5CX Dual Beam system. AFM images were analyzed on Bruker Nanowizard 4XP Atomic Force Microscope. SEM images were collected by JEOL JSM-7900F field emission scanning electron microscope.

Preparation of Zn-VBA

500 mg zinc oxide (ZnO) was dispersed in 10 mL of fluorobenzene by vigorously stirring and heating at 60 °C. The organic ligand, 4-vinylbenzoic acid (390 mg) was also dissolved in 10 mL of fluorobenzene by heating at 70 °C. Then the ZnO dispersion was added to the 4-vinylbenzoic acid solution, and the reaction mixture was refluxed under a nitrogen atmosphere until the reaction completed for 24 h at 84 °C. 20 mL of fluorobenzene were added after cooling to 60 °C. Then the reaction mixture was filtered, and the filtrate was dried to remove the excess solvent. The white residue was recrystallized from 10:1 to 10:5 toluene (good solvent) / hexane (non-solvent) at 80 °C, and cooled to room temperature to yield a transparent crystalline solid (380 mg , yield 74.72%). Other zinc oxide clusters are synthesized and recrystallized similarly.[1]

Zn-VBA: ^{1}H NMR (500 MHz, Chloroform-*d*, ppm) δ 8.08 (d, J = 8.1 Hz, 12H), 7.49 (d, J = 8.2 Hz, 12H), 6.77 (dd, J = 17.6, 10.9 Hz, 6H), 5.89 (d, J = 17.6 Hz, 6H), 5.41 (d, J = 11.0 Hz, 6H).
^{13}C NMR (101 MHz, DMSO-d_6, ppm) δ 167.10, 141.35, 135.90, 130.01, 129.72, 126.27, 117.02.
Elemental analysis (%) for $C_{54}H_{42}O_{13}Zn_4$ calc.: C, 55.89; H, 3.65; found: C, 56.33; H, 3.78.
ICP (%) for $C_{54}H_{42}O_{13}Zn_4$ calc.:Zn, 22.54; found: 20.01.
ESI-MS: $[M+L]^-$=$[(CH_2CHC_6H_4COO)_6OZn_4+ CH_2CHC_6H_4COO]^-$:
Anal:1307.0130, found:1307.0409.

Zn-TBA：^{1}H NMR (400 MHz, Chloroform-*d*, ppm) δ 8.35 (d, *J* = 8.1 Hz, 12H), 7.73 (d, *J* = 8.2 Hz, 12H).
^{13}C NMR (126 MHz, Chloroform-*d*, ppm) δ 174.98, 135.64, 134.73 (q, *J* = 32.5 Hz)., 131.24, 125.30, 123.79(q, *J* = 272.1Hz).
^{19}F NMR (376 MHz, Chloroform-*d*, ppm) δ -63.06.
Elemental analysis (%) for $C_{48}H_{24}F_{18}O_{13}Zn_4$ calc.: C, 40.82; H, 1.71; found: C, 41.98; H, 1.68.
ICP (%) for $C_{48}H_{24}F_{18}O_{13}Zn_4$ calc.:Zn, 18.52;found: 15.90.
ESI-MS: $[M+L]^-$=$[(CF_3C_6H_4COO)_6OZn_4+CF_3C_6H_4COO]^-$:
Anal:1600.8152, found:1600.8112.

Zn-BA：^{1}H NMR (400 MHz, Chloroform-*d*, ppm) δ 8.24 – 8.19 (m, 12H), 7.52 (t, *J* =

7.4 Hz, 6H), 7.42 (t, J = 7.6 Hz, 12H).

^{13}C NMR (101 MHz, DMSO-d_6, ppm) δ 171.84, 134.75, 130.99, 129.57, 127.94.

Elemental analysis (%) for $C_{42}H_{30}O_{13}Zn_4$ calc.: C, 50.23; H, 3.01; found: C,50.52; H, 2.82.

ICP (%) for $C_{42}H_{30}O_{13}Zn_4$ calc.:Zn, 26.04; found: 22.16.

ESI-MS: $[M+L]^-=[(C_6H_5COO)_6OZn_4+ C_6H_5COO]^-$

Anal:1124.9035, found:1124.9281.

Single crystal X-ray crystallography

X-Ray intensity data of Zn-**VBA and** Zn-**TBA** were measured on a Bruker SMART APEX CCD-based diffractometer (Mo–Kα radiation, λ = 0.71073 Å) using the SMART and SAINT programs.[2][3] Using Olex2[4], The crystal data were solved by direct methods and further refined by full-matrix least-squares refinements on F^2 using the SHELXL-2018 software. CCDC 2215806 for Zn-**VBA** and CCDC 2225688 for Zn-**TBA** contain the supplementary crystallographic data for this paper. The data can be obtained free of charge from the Cambridge Crystallographic Data Centre via www.ccdc.cam.ac.uk/data_request/cif.

Computational calculations

The structures of Zn-**VBA**, Zn-**BA** and Zn-**TBA** were optimized using functional theory (DFT) with the hybrid B3LYP functional. The 6-31g(d) basis set was selected for H, C, O atoms and Stuttgart pseudopotentail and basis set (SDD) was used for Zn atom. The NBO (natural bond orbital) calculations were carried out based on the optimized structures. The geometry optimization of solvent molecules were performed by DFT at B3LYP/6-311++G(d,p) level. The ESP calculations were performed at the same theoretical level and shown using GaussView 6.0. All calculations were done with the Gaussian 16 package [5], Revision C.01.

Solubility test

The solubility of photoresist was evaluated by the mass of dissolution per unit volume and the dissolution rate as a whole, and the film-forming property was evaluated by atomic force microscope.

EBL test

Zn-**VBA** photoresist solution (30 mg/mL) was prepared in cyclohexanone followed by filtration using a 0.22 μm PTFE filter. Thin films were prepared by spin-coating the resist solution on a 1×1 cm^2 silicon substrate at 3000 rpm for 30 s. Post-application baking (PAB) was applied for 60 s at 90 °C to remove excess residual solvent. The morphology and thickness of the coated films were measured by AFM and ellipsometry. Then the films were exposed at various doses at 30 keV (5 μC/cm^2 and 20 μC/cm^2) with a 264 pA beam current. After exposure, the film-coated wafers were developed for 30 seconds by MIBK: IPA = 1:3 at 25 °C and then rinsed for 5 seconds in deionized water before drying.

Zn-**VBA** photoresist solution (20 mg/mL) was prepared in PGMEA and Zn-**TBA** photoresist solution (40 mg/mL) was prepared in chlorobenzene followed by filtration using 0.22 μm PTFE filter. Thin films were prepared by spin-coating the resist solution on a 1×1 cm^2 silicon substrate at 5000 rpm for 60 s separately. The films were exposed at various doses at 25 keV with a 665 pA beam current (20 μC/cm^2 for Zn-**VBA** and 550 μC/cm^2 for Zn-**TBA**). After exposure, the Zn-**VBA** film-coated wafers were developed for 30 seconds by MIBK: IPA = 1:3 at 25°C and then rinsed for 5 seconds in deionized water before drying. And the Zn-**TBA** film-coated wafers were developed for 30 seconds by n-hexane at 25°C and then rinsed for 2 seconds in deionized water before drying.

EUVL test

The 30 mg/mL resist solutions were spin-coated onto a 2 in. silicon wafer leading to the formation of uniform films in the thickness of approximately 35-40 nm. The film-coated wafers were subjected to a PAB at 90 °C for 60 s and then exposed to EUV by using a soft X-ray interference photolithography beamline in Shanghai Synchrotron Radiation Facility (SSRF). The area of interference was approximately 100×100 μm^2. After exposure, the film-coated wafers were developed for 30 seconds by MIBK: IPA = 1:3 at 25°C and then rinsed for 5 seconds in deionized water before drying.
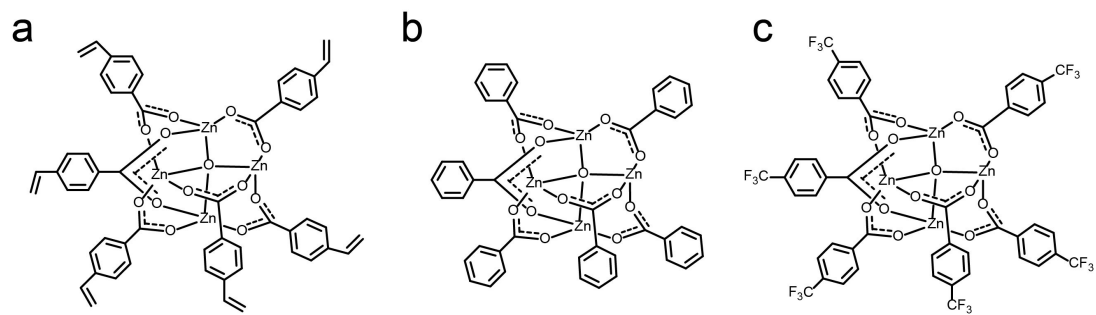
Fig S1. Chemical structures of (a) Zn-**VBA**, (b) Zn-**BA** and (c) Zn-**TBA** clusters.
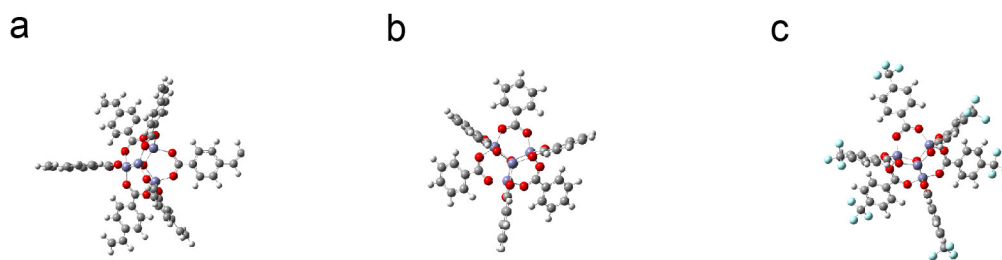
Fig S2. Structural optimization of (a) Zn-**VBA**, (b) Zn-**BA** and (c) Zn-**TBA** clusters.
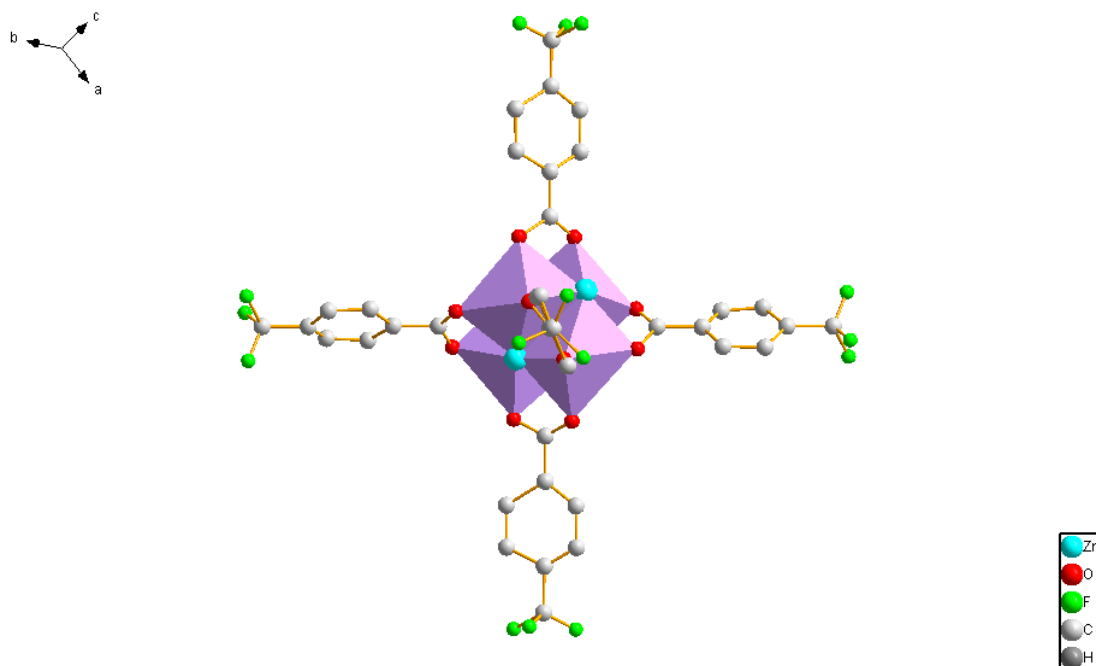
Fig S3. Single-crystal X-ray diffraction structure of Zn-**TBA**.

Table S1. Crystallographic data structure refinement for Zn-VBA.

Compound	Zn-**VBA**
Formula	$C_{115}H_{92}O_{26}Zn_8$
Formula weight	2412.84
Temperature/K	120.00
Crystal system	Monoclinic
Space group	$P2_1/n$
a/Å	23.6140(10)
b/Å	16.3125(6)
c/Å	28.0058(11)
α/°	90
β/°	94.1020(10)
γ/°	90
Volume/Å^3	10760.3(7)
Z	4
$\rho_{calc}g/cm^3$	1.489
μ/mm^{-1}	1.825
F(000)	4920.0
Radiation	MoKα (λ = 0.71073)
2Θ range for data collection/°	4.296 to 50
Index ranges	$-28 \leq h \leq 28$, $-19 \leq k \leq 18$, $-33 \leq l \leq 31$
Reflections collected	74819
Completeness to theta	25.000,99.9%
Independent reflections	18924 [R_{int} = 0.1204]
Data/restraints/parameters	18924/610/1515
Goodness-of-fit on F^2	1.012
Final R indexes [I>=2σ (I)]	R_1 = 0.0598, wR_2 = 0.1366
Final R indexes [all data]	R_1 = 0.1320, wR_2 = 0.1785
Largest diff. peak/hole / e Å^{-3}	0.88/-0.88
CCDC No.	2215806

Table S2. Crystallographic data structure refinement for Zn-TBA.

Compound	Zn-**TBA**
Formula	$C_{48}H_{24}F_{18}O_{13}Zn_4$
Formula weight	1412.15
Temperature/K	150.00
Crystal system	Trigonal
Space group	R-3
a/Å	22.863(3)
b/Å	22.863(3)
c/Å	8.616(4)
α/°	90
β/°	90
γ/°	120
Volume/Å^3	3900.5(19)
Z	3
ρ_{calc}g/cm^3	1.804
μ/mm^{-1}	1.950
F(000)	2094.0
Radiation	MoKα (λ = 0.71073)
2Θ range for data collection/°	5.156 to 52.662
Index ranges	-28 ≤ h ≤ 26, -28 ≤ k ≤ 24, -10 ≤ l ≤ 9
Reflections collected	10428
Completeness to theta	25.621,99.9%
Independent reflections	1766 [R_{int} = 0.1568]
Data/restraints/parameters	1766/50/205
Goodness-of-fit on F^2	1.090
Final R indexes [I>=2σ (I)]	R_1 = 0.0853, wR_2 = 0.1553
Final R indexes [all data]	R_1 = 0.1547, wR_2 = 0.1802
Largest diff. peak/hole / e Å^{-3}	0.62/-0.49
CCDC No.	2225688

Table S3. Solubility and film-forming property test of Zn-VBA.

solvent	solubility	film-formation
toluene	++	+++
chlorobenzene	+++	+
Fluorobenzene	+++	+
Dichloroethane	+++	+++
PGMEA	+++	+++
PGME	+++	++
EGME [a]	+++	+
EAME [b]	++	+
EGDE [c]	+++	+
DGDE [d]	++	+
ethyl lactate	+++	++++
tert-butanol	-	-
acetone	+++	+++
cyclohexanone	+++	++++
ethanol	+	
water	-	

[a] EGME (2-ethoxyethanol) [b] EAME (2-Methoxyethanol) [c] EGDE (1,2-Dimethoxyethane)

[d] DGDE (Diethylene glycol dimethyl ether)

"+"Indicates positive correlation and "-" conversely.

Solubility: +++ indicate above 30 mg/mL , ++ indicate 20-30 mg/mL , + indicate less than 10 mg/mL , - indicate insoluble.

Film-formation: ++++ indicate Rq within 0.3 nm , +++ indicate Rq within 1.0 nm , ++ indicate Rq within 5.0 nm , + indicate Rq within 10.0 nm ; - indicate poor film-formation.
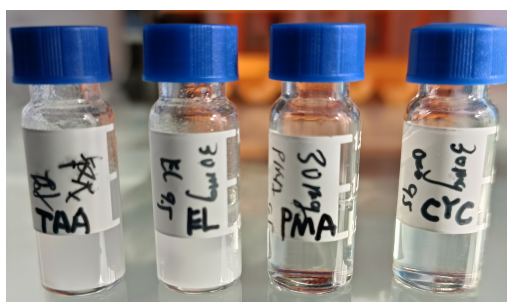
Fig S4. The photo of Zn-**VBA** (30 mg/mL) in different solutions (tert-butanol, ethyl lactate, PGMEA and cyclohexanone) keeping at room temperature for one week.
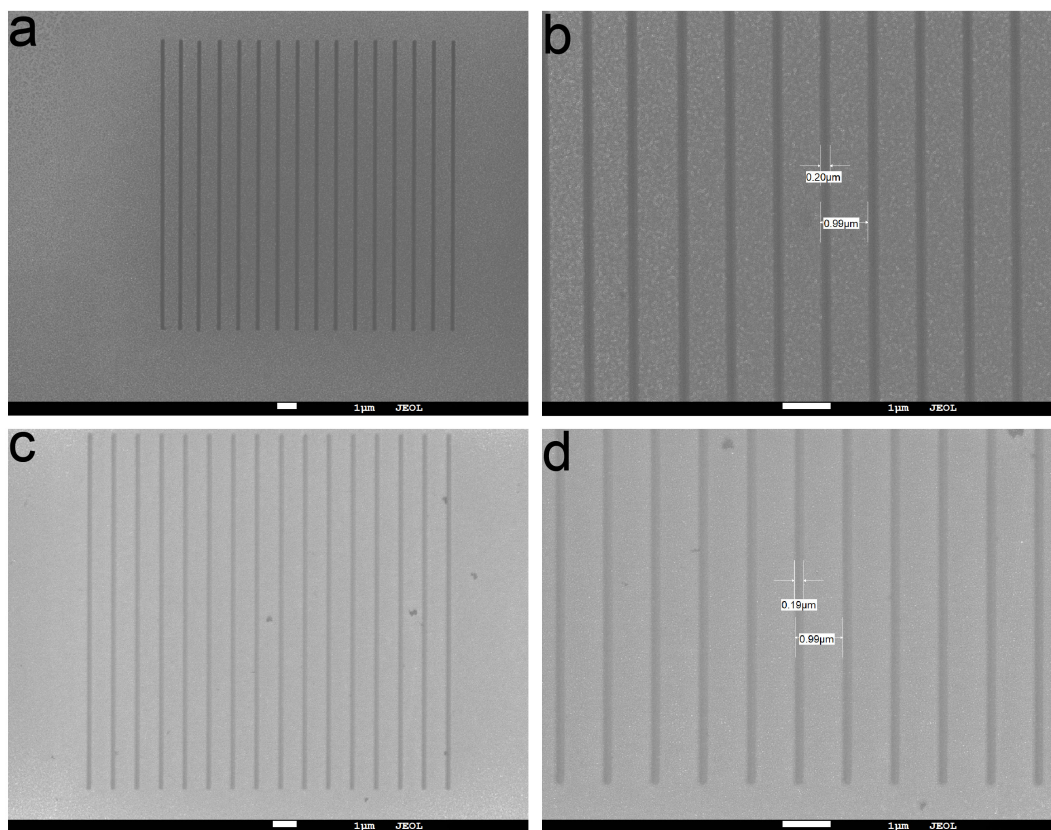
Fig S5. FE-SEM images of Zn-**VBA** resist patterning upon exposure by EBL. (a) ×5500 (5 µC/cm^2). (b) ×11000 (5 µC/cm^2). (c) ×5500 (20 µC/cm^2) and (d) ×11000 (20 µC/cm^2).
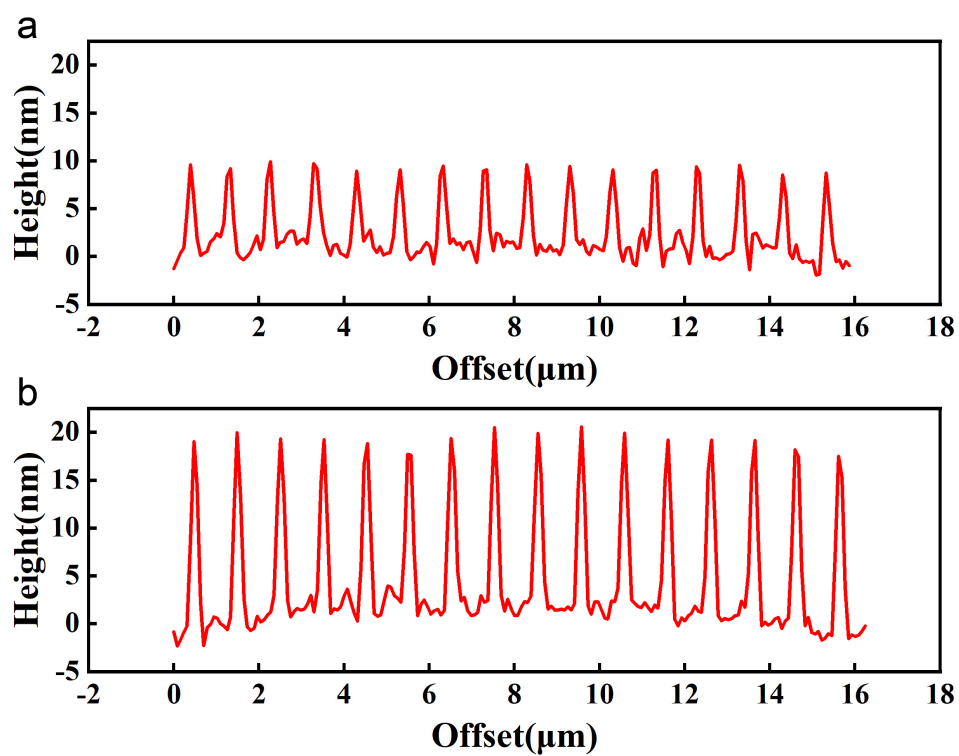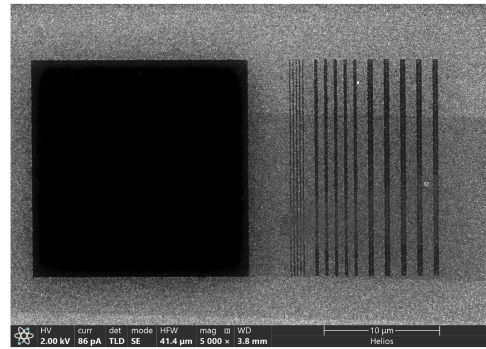

Fig S6. The section profiles of the AFM images of Zn-**VBA** resists patterned by EBL
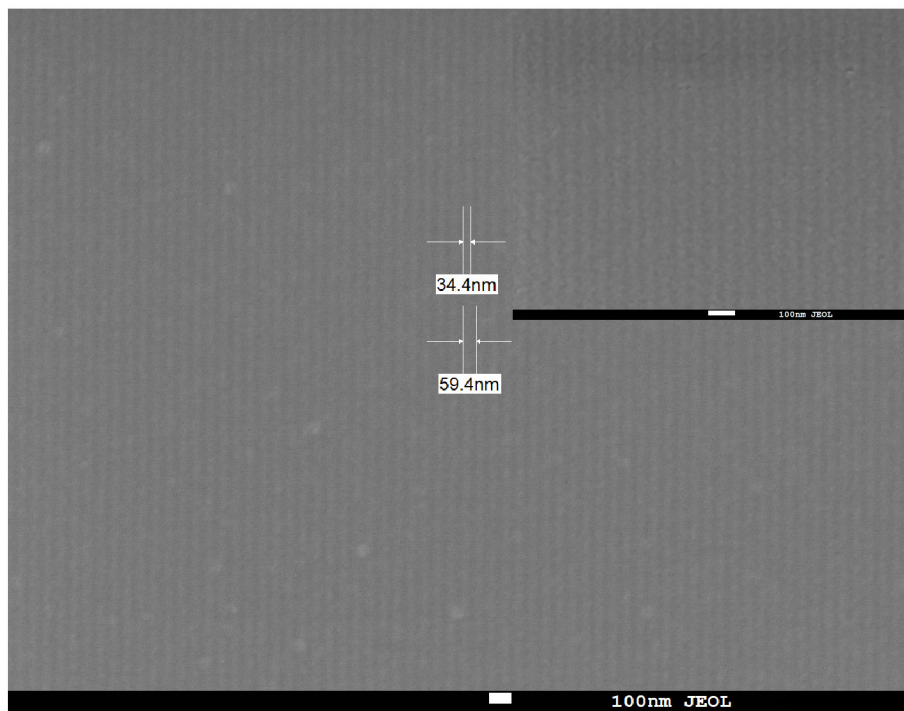
at the dose of (a) 5 µC/cm^2 and (b) 20 µC/cm^2.

a
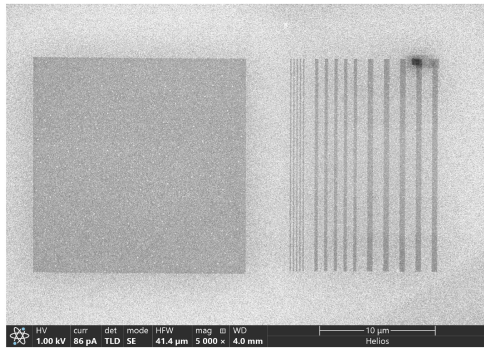
b

Fig S7. SEM images of the patterns formed upon EBL exposure of (a) 20 µC/cm^2 for Zn-**VBA** resist and (b) 550 µC/cm^2 for Zn-**TBA** resist at 25 keV.

Fig S8. Zn-**VBA** resist patterned by EUV lithography (92.5 mJ/cm^2) performed with 60 nm pitch.
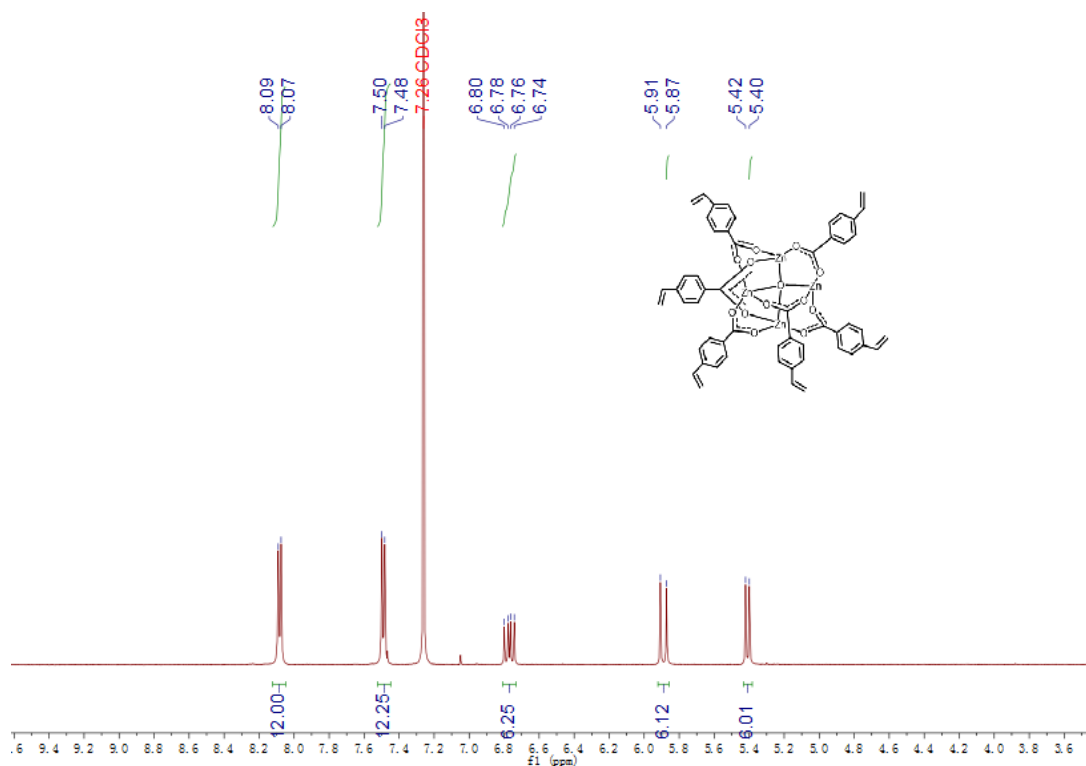
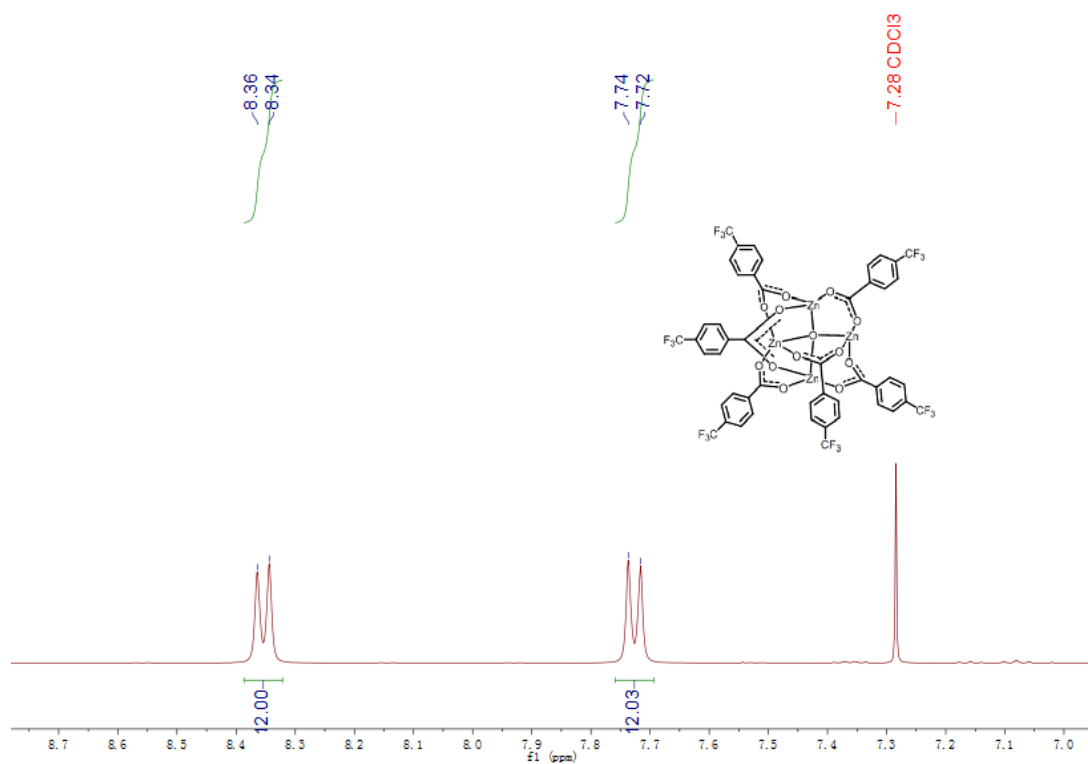**Fig S9**. ^{1}H NMR spectrum of Zn-**VBA** in chloroform-*d*.
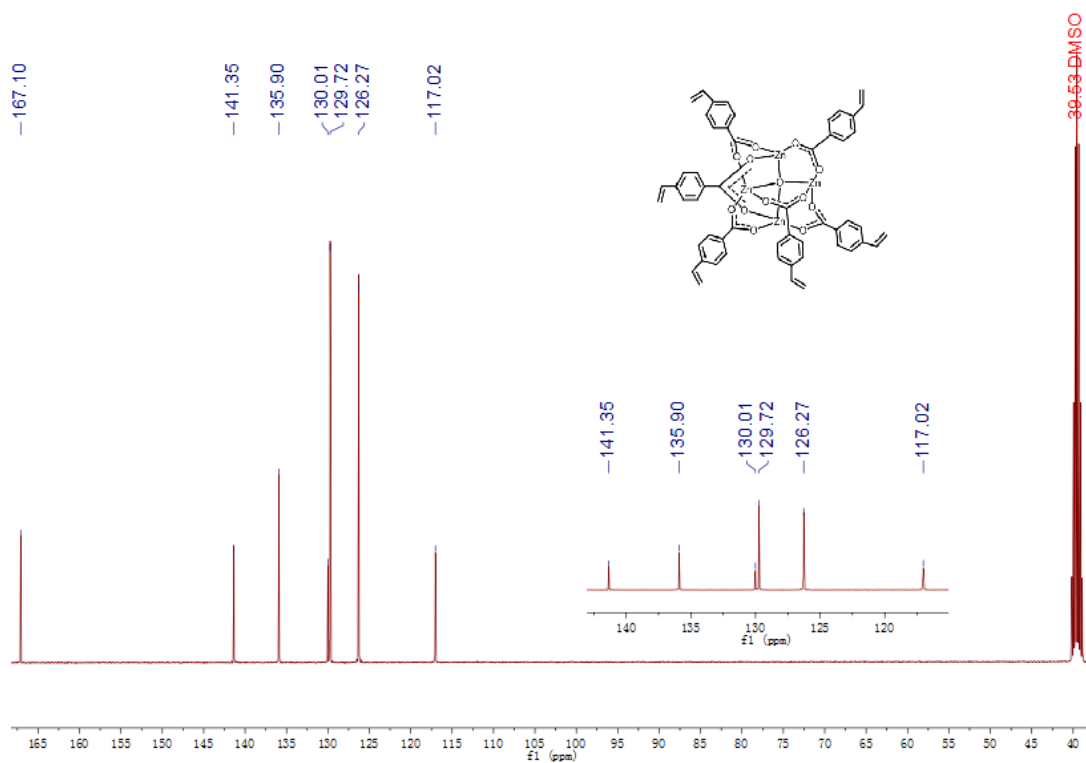
Fig S10. ^{13}C NMR spectrum of Zn-**VBA** in DMSO-*d*$_6$.
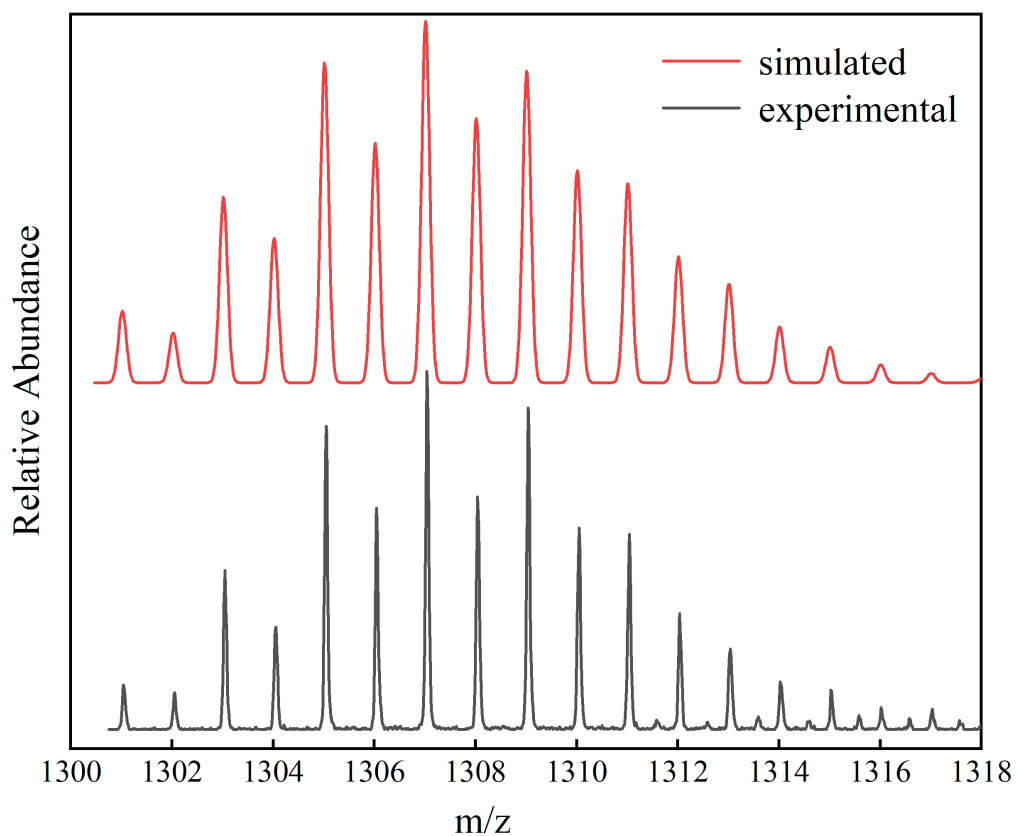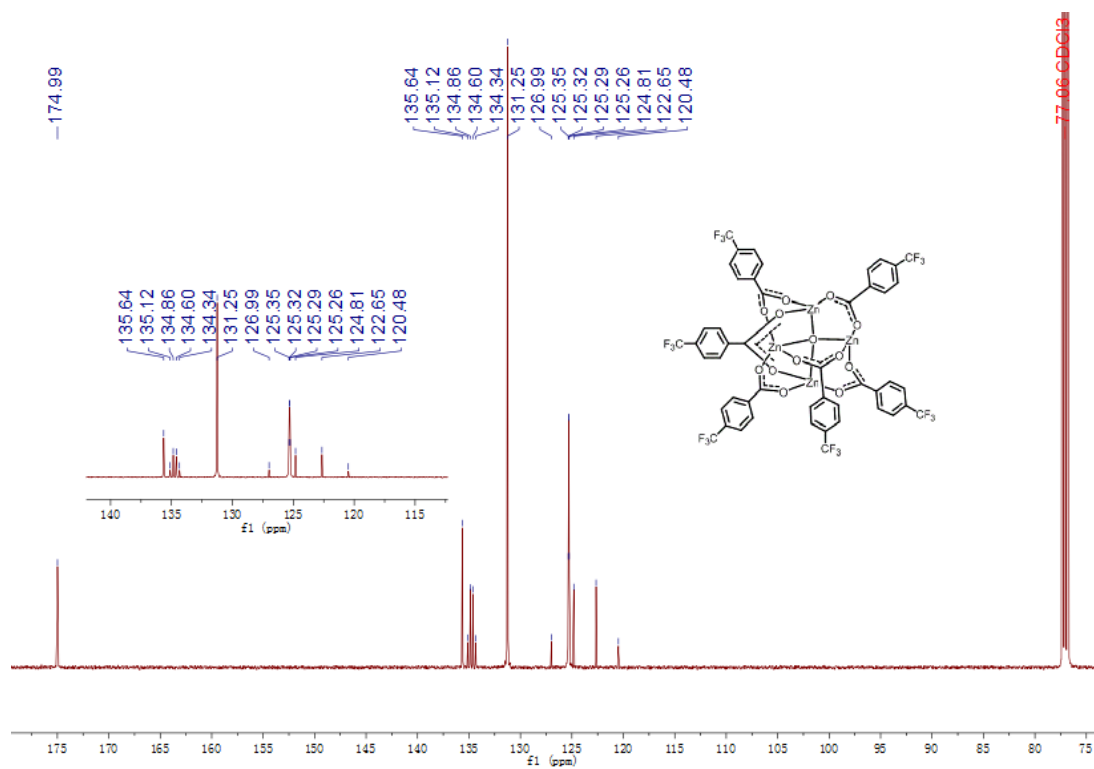
Fig S11. The experimental and simulated patterns of the negative ESI-MS spectrum of Zn-**VBA** in CH_2Cl_2.

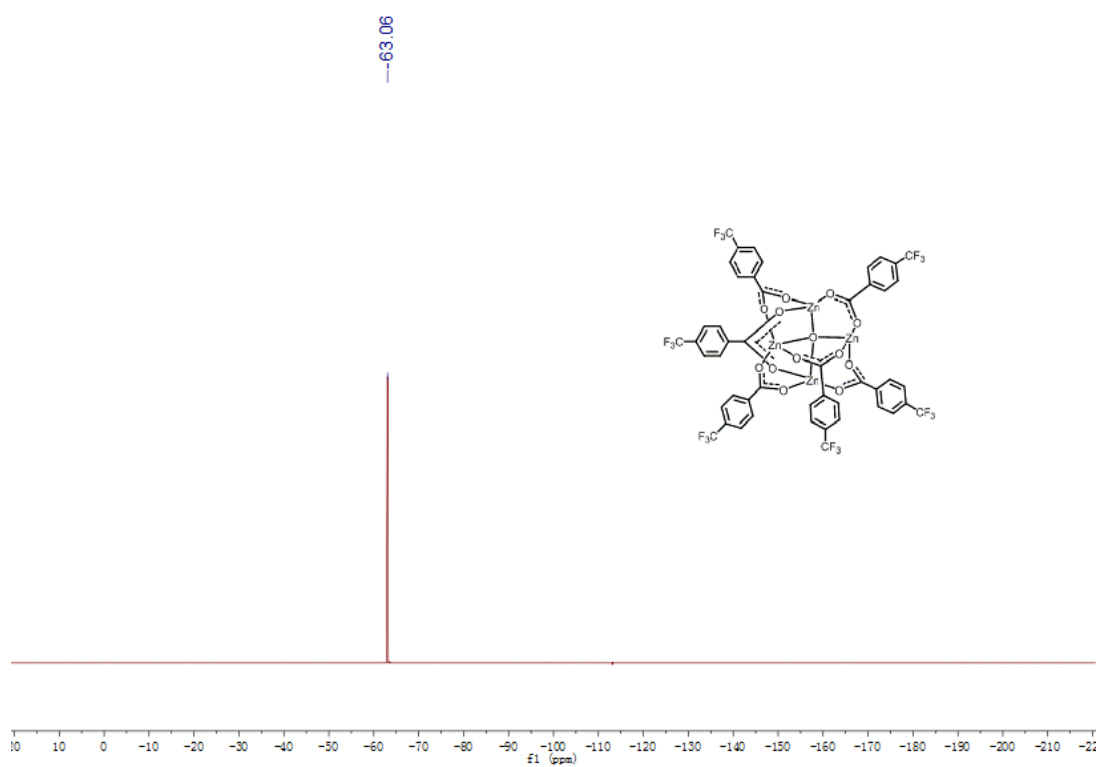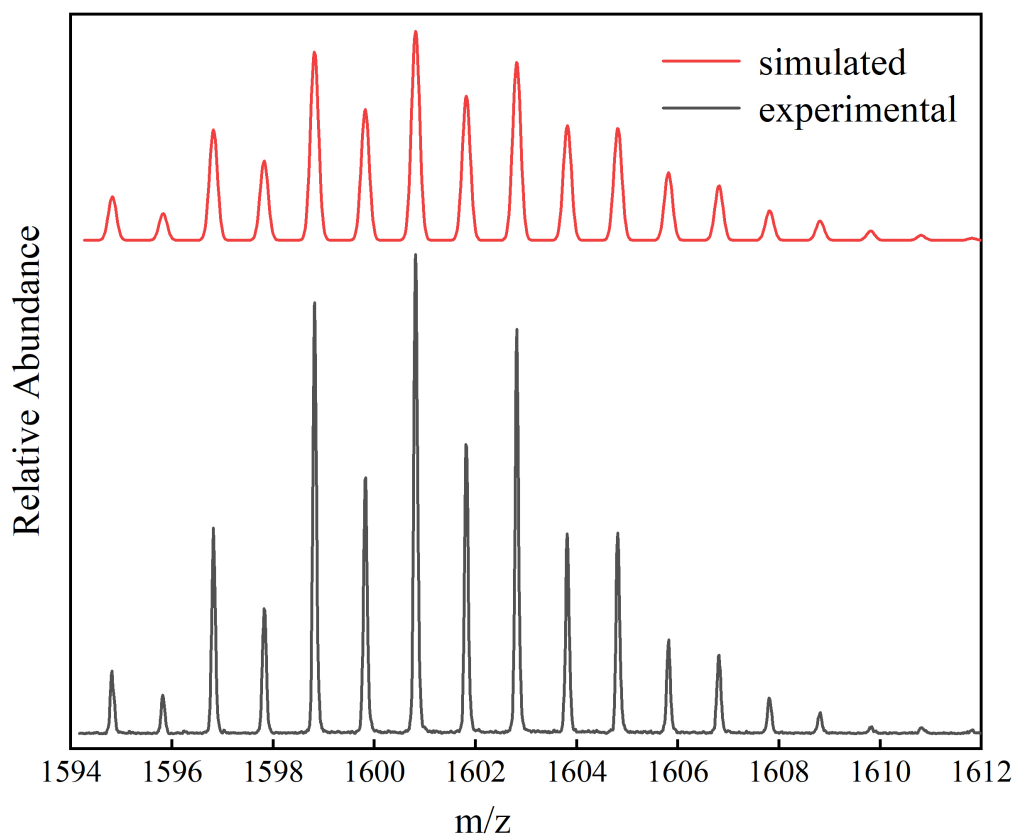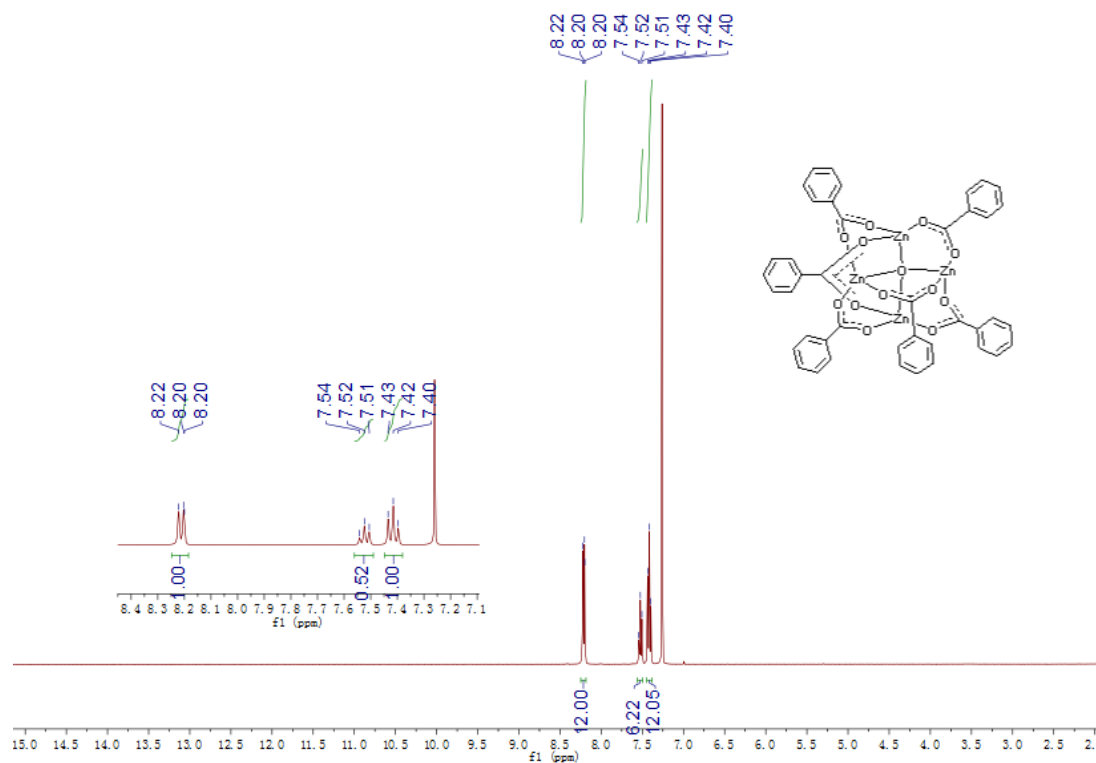**Fig S12**. ^{1}H NMR spectrum of Zn-**TBA** in chloroform-*d*.

Fig S13. ^{13}C NMR spectrum of Zn-**TBA** in chloroform-*d*.

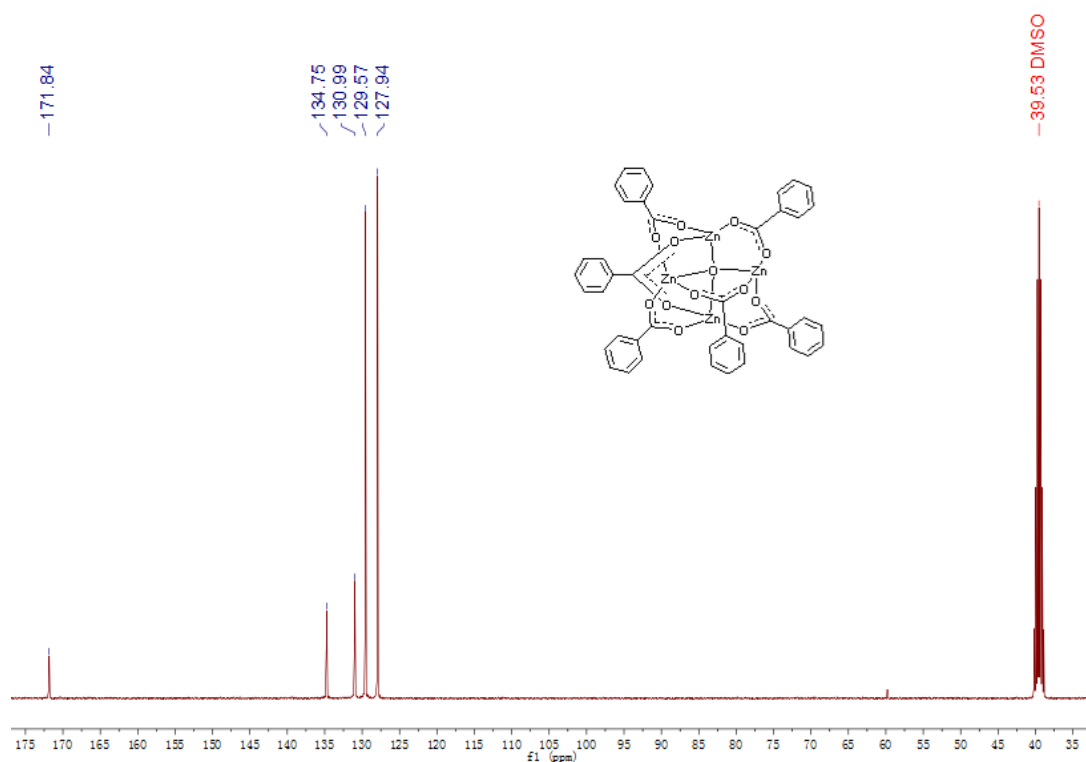**Fig S14**. ^{19}F NMR spectrum of Zn-**TBA** in chloroform-*d*.
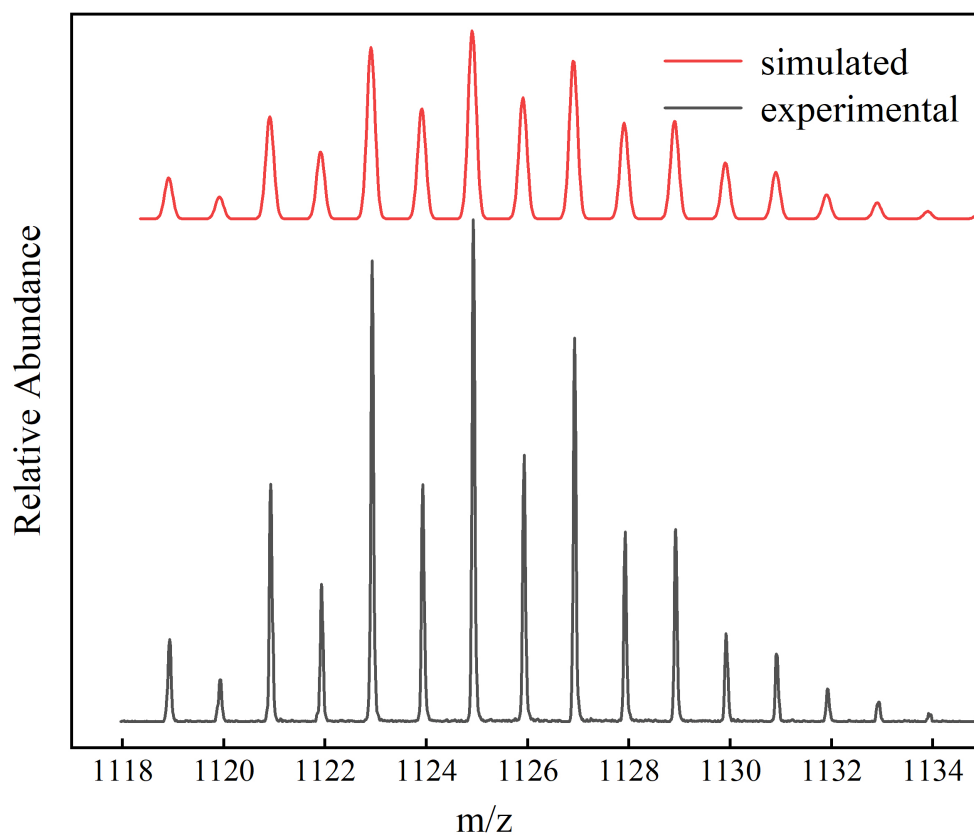
Fig S15. The experimental and simulated patterns of the negative ESI-MS spectrum of Zn-**TBA** in CH$_2$Cl$_2$.

Fig S16. ^{1}H NMR spectrum of Zn-**BA** in chloroform-d.

Fig S17. ^{13}C NMR spectrum of Zn-**BA** in DMSO-d_6.

Fig S18. The experimental and simulated patterns of the negative ESI-MS spectrum of Zn-**BA** in CH$_2$Cl$_2$.

Supporting References

[1]   W. Clegg, D. R. Harbron, C. D. Homan, P. A. Hunt, I. R. Little and B. P. Straughan, *Inorganica Chimica Acta*, 1991, **186**, 51-60.

[2]   SMART Data collection software, version 5.629; Bruker AXS Inc.: Madison, WI, 2003.

[3]   SAINT Data reduction software, version 6.45; Bruker AXS Inc.: Madison, WI, 2003.

[4]   O. V. Dolomanov, L. J. Bourhis, R. J. Gildea, J. A. K. Howard and H. J. J. o. A. C. Puschmann, 2009, 42, 339-341.

[5]   M. J. Frisch, G. W. Trucks, H. B. Schlegel, G. E. Scuseria,   M. A. Robb, J. R. Cheeseman, G. Scalmani, V. Barone,   G. A. Petersson, H. Nakatsuji, X. Li, M. Caricato, A. V. Marenich,   J. Bloino, B. G. Janesko, R. Gomperts, B. Mennucci, H. P. Hratchian,   J. V. Ortiz, A. F. Izmaylov, J. L. Sonnenberg, D. Williams-Young,   F. Ding, F. Lipparini, F. Egidi, J. Goings, B. Peng, A. Petrone,   T. Henderson, D. Ranasinghe, V. G. Zakrzewski, J. Gao, N. Rega, G. Zheng, W. Liang, M. Hada, M. Ehara, K. Toyota, R. Fukuda,   J. Hasegawa, M. Ishida, T. Nakajima, Y. Honda, O. Kitao, H. Nakai,   T. Vreven, K. Throssell, J. A. Montgomery, Jr., J. E. Peralta,   F. Ogliaro, M. J. Bearpark, J. J. Heyd, E. N. Brothers, K. N. Kudin,   V. N. Staroverov, T. A. Keith, R. Kobayashi, J. Normand,   K. Raghavachari, A. P. Rendell, J. C. Burant, S. S. Iyengar,   J. Tomasi, M. Cossi, J. M. Millam, M. Klene, C. Adamo, R. Cammi, J. W. Ochterski, R. L. Martin, K. Morokuma, O. Farkas,   J. B. Foresman, and D. J. Fox, Gaussian, Inc., Wallingford CT, 2019.